Applied Clay Science xxx (2016) xxx–xxx

Contents lists available at ScienceDirect

Applied Clay Science

journal homepage: www.elsevier.com/locate/clay

Research paper

Reduction of filler networking in silica based elastomeric nanocomposites with exfoliated organo-montmorillonite

Maurizio Galimberti [a,*], Valeria Cipolletti [a,1], Serena Cioppa [a], Angela Lostritto [b], Lucia Conzatti [c]

[a] Politecnico di Milano, Via Mancinelli 7, 20131 Milano, Italy
[b] Pirelli Tyre SpA, Viale Sarca 222, 20126 Milano, Italy
[c] Consiglio Nazionale delle Ricerche, Istituto per lo Studio delle Macromolecole, Via De Marini 6, 16149 Genova, Italy

ARTICLE INFO

Article history:
Received 15 June 2016
Received in revised form 12 September 2016
Accepted 12 September 2016
Available online xxxx

Keywords:
Silica
Montmorillonite
Organoclay
Nanocomposite
Filler networking

ABSTRACT

Montmorillonite with dimethyl di(hydrogenatedtalloyl) ammonium as the compensating cation was added to a silica based elastomeric composite and the hybrid filler system led to reduction of filler networking phenomenon, better stability of elastic modulus with temperature, enhancement of stresses at all elongations, improvement of ultimate properties. This composite was based on a blend of natural rubber, poly(1,4-*cis*-isoprene) and poly(styrene-*co*-butadiene) from anionic polymerization and contained 70 parts per hundred rubber (phr) of silica. The organically modified clay (OC) was below the threshold required to establish an hybrid OC-silica filler network. Such threshold (about 7 phr) was estimated by preparing silica based nanocomposites containing various amounts of OC and determining shear storage and loss moduli as a function of strain amplitude. This work demonstrates that exfoliated OC favour lower dissipation of energy of silica based elastomeric composites under dynamic mechanical stresses and paves the way for further large scale applications.

1. Introduction

Silica is characterized by the polar surface rich of oxygen atoms, involved in siloxane and silanol functional groups (Legrand, 1998). Precipitated silica (Chevalier and Morawski, 1984; Legrand, 1998), having high specific surface area and activity, has thus poor dispersibility in apolar matrices and easily forms filler networks in polymer melts and elastomers (Donnet and Custodero, 2005). Compatibilization of precipitated silica with hydrocarbon polymers is achieved by using molecules, such as organosilanes, that react with silanols, shielding the silica surface and that, in some cases, form covalent bonds with the polymer chains (Leblanc, 2002; Donnet and Custodero, 2005; Fröhlich et al., 2005). Composites based on diene elastomers, precipitated silica and organosilanes reactive with the polymer are the preferred ones for large scale highly demanding dynamic-mechanical applications such as the one in tyre compounds, when low dissipation of energy is required (Leblanc, 2002; Donnet and Custodero, 2005; Fröhlich et al., 2005). In fact, the efficient distribution and dispersion of the silica/silane system and its interaction with the polymer matrix substantially reduce the filler networking phenomenon, that is known as the main source of energy dissipation. The most important application of precipitated silica is indeed in the field of elastomeric composites. Research is continuously performed both in academic and industrial laboratories in order to achieve further reduction of the filler networking in such silica based composites.

Cationic clay minerals (Bergaya and Lagaly, 2013) have been widely used over the last decades for the preparation of both thermoplastic and elastomeric composite materials (LeBaron et al., 1999; Alexandre and Dubois, 2000; Ray and Okamoto, 2003; Annabi-Bergaya, 2008; Chen et al., 2008; Galimberti, 2011a). Their compatibilization with apolar polymer matrices is successfully achieved through the exchange reaction of the alkali and alkali-earth cations with organophilic ammonium salts (Lagaly et al., 2013). Clay polymer nanocomposites (CPN) containing the organically modified clays (OC) are characterized by improved mechanical reinforcement, impermeability and thermal stability (Paul and Robeson, 2008; Galimberti et al., 2013a). It is also acknowledged that OC give rise to remarkable filler networking in polymer melts and elastomers (Ramorino et al., 2009; Galimberti et al., 2011b; Galimberti et al., 2012), that means to pronounced Payne effect (Payne, 1962). The addition of OC to silica based composites could thus improve important properties, but could also lead to an undesired enhancement of filler networking phenomenon.

It is thus worthwhile to study the filler networking phenomenon and the static and dynamic-mechanical properties of polymer melts and elastomers based on silica and OC. In the scientific literature, many papers are available on elastomeric nanocomposites based on OC and carbon black (CB) (Maiti et al., 2005; Cataldo, 2007; Praveen et al., 2009; Galimberti et al., 2009, 2012, 2013b; Sridhar et al., 2009; Das

* Corresponding author.
E-mail address: maurizio.galimberti@polimi.it (M. Galimberti).
[1] Present address: Pirelli Tyre, Viale Sarca 222, 2016 Milano, Italy.

http://dx.doi.org/10.1016/j.clay.2016.09.017
0169-1317/

et al., 2010; Chattopadhyay et al., 2011; Gopi et al., 2011; Malas and Das, 2012). It has been shown that OC favours the filler networking phenomenon, leading to the formation of hybrid OC-CB filler networks (Galimberti et al., 2012, 2013b).

The intimate interaction between CB and a nanofiller has been justified on the basis of the zeta potential (ZP) values (Bhattacharya and Bhowmick, 2010): in the pH range of elastomeric composite, ZP of CB is positive, whereas those of nanofillers are negative (Gates, 2004; Lin et al., 2006; Sabah et al., 2007; Xu et al., 2007; Kvande et al., 2008). It was commented that ZP can be also applied to polymer melts (Brochard-Wyart and de Gennes, 2000; Flores et al., 2007) and the affinity of clay minerals for CB was reported (Feller et al., 2004; Konishi and Cakmak, 2005; Galimberti et al., 2012).

The affinity of clay minerals for silica is intuitive. Moreover, positive values of ZP have been reported for silica (Anderson and Zukoski, 2007). The addition of OC to silica based composite could thus lead to the enhancement of the filler networking phenomenon. Only a few papers are available on elastomeric CPN containing silica and OC: they are based on poly(1,4-cis-isoprene) from *Hevea brasiliensis* (natural rubber, NR) (Rattanasom and Prasertsri, 2012) and poly(styrene-*co*-butadiene) (SBR) (Kim et al., 2009, 2011, 2013). The presence of OC was shown to enhance the tensile moduli and to worsen the ultimate properties (Kim et al., 2011) and it was reported that OC does not form filler–filler networks with silica (Kim et al., 2013). The amount of OC was kept constant and the content of silica was not higher than 53 parts per hundred rubber (phr) (Kim et al., 2013).

Aim of this work was to study the filler networking phenomenon in elastomeric nanocomposites containing precipitated silica and OC. Montmorillonite (Mt) with dimethyl di-hydrogenated talloyl (2HT) as the compensating cation was used as the OC. Poly(1,4-cis-isoprene) from Ziegler-Natta catalysis (PI) and a blend of PI, SBR and poly(1,4-cis-butadiene) were used as the polymer matrix and nanocomposites were prepared via melt blending. Structure of nanocomposites containing OC and silica was investigated by means of transmission electron microscopy (TEM) and X-ray diffraction (XRD) analysis. Dynamic-mechanical moduli were determined through measurements in the torsion and in the axial mode. Stresses at various elongations and ultimate properties were assessed with quasi-static measurements.

2. Experimental

2.1. Materials

2.1.1. Organoclay and ammonium salt

OC was Mt with dimethyl di(hydrogenated talloyl) ammonium (2HT) as the compensating cation (Dellite® 67G from Laviosa Chimica Mineraria S.p.A.). Mt and the ammonium moiety were 55 and 45 as mass %, respectively. The ammonium salt was dimethyl di-hydrogenated talloyl ammonium chloride (2HTCl) (Arquad® HC Pastilles from Akzo Nobel). Typical value of chemical purity was 98.5 mass %. The alkyl chain distribution, as mass%, was: $<C_{12} = 1$, $C_{14} = 4$, $C_{16} = 31$, $C_{18} = 64$.

2.1.2. Silica

Precipitated silica was Ultrasil 7000 from Evonik, with 270 g/L density and 175 m^2/g as specific surface area, determined through nitrogen absorption.

2.1.3. Polymers

Synthetic poly(1,4-*cis*-isoprene) (PI) (SKI3 from Nizhnekamskneftechim Export) had 70 Mooney Units (MU) as Mooney viscosity ($M_{L(1+4)}$ at 100 °C). Poly(1,4-*cis*-butadiene) (BR) (Buna CB 25 from Lanxsess) had 44 MU as Mooney viscosity ($M_{L(1+4)}$ at 100 °C). Poly(styrene-*co*-butadiene) from anionic solution polymerization (sSBR) (SOL R 72612 from Versalis) had 25 mass% of styrene, 50 mass% of vinyl groups, 36.8 phr of aliphatic extension oil and 48 MU as Mooney viscosity ($M_{L(1+4)}$ at 100 °C).

2.1.4. Other ingredients for composites preparation

Aliphatic oil catenex SNR was from Shell; bis(triethoxysilylpropyl) tetrasulfide (TESPT) (Si69) was from Evonik. ZnO was from Zincol Ossidi; stearic acid (chemical composition: C16 + C18 = 95 mass%, C12 + C14 = 5 mass%) was from Sogis. *N*-(1,3-dimethylbutyl)-*N*′-phenyl-*p*-phenylendiamine (6PPD) was from Flexsys, 2,5-dimethyl-2,5-di(*t*-butylperoxy)hexane (DCUP) supported on Silica/$CaCO_3$ (45 mass%) was from Arkema Inc., and sulphur was from Solfotecnica. Benzothiazyl-2-cyclohexylsulfenamide (CBS), diphenyl guanidine (DPG), and *N*-(cyclohexylthio)phthalimide (CTP), were from Flexsys.

2.2. Preparation of composites and nanocomposites

2.2.1. PI based nanocomposites containing silica and OC

Formulations are in Table 1. A PI/silica masterbatch was firstly prepared. In the first step of the procedure, 738 g of PI were introduced into the Banbury® type internal mixer (1050 mL mixing chamber) at 60 °C and masticated for 30 s with rotors rotating at 75 rpm. In the second step, 517 g of silica and 51.7 g of TESPT were added, temperature was rapidly increased to 150 °C, mixing was carried out for further 240 s and the resulting PI/silica masterbatch was discharged at 150 °C. This masterbatch was then used for the preparation of all the nanocomposites. For the composite with only silica as the filler (OC-0), the PI/silica masterbatch was introduced into the Brabender® type internal mixer (50 mL mixing chamber) and peroxide was added, performing the mixing at 50 °C for 120 s. For the nanocomposites containing silica and OC, the PI/silica masterbatch was introduced into the Brabender® type internal mixer at 80 °C and masticated at 30 rpm for 60 s. OC was then added and mixing was carried out for 240 s, discharging the nanocomposite at about 90 °C. The nanocomposite with OC was finally fed at room temperature to the Brabender® mixer and the peroxide was added, performing the mixing at 50 °C for 120 s. Curing was carried out at 170 °C for 20 min under a pressure of 150 bar. Nanocomposites were labelled as OC-X, where X indicates the amount of OC expressed in phr (part per hundred rubber).

2.2.2. PI based composites containing silica and 2HTCl

The same formulations reported in Table 1 were adopted, except that in place of OC a molar amount of 2HTCl equal to the molar amount of 2HT in OC was added. The amounts of 2HTCl in phr were: 0.22, 0.49, 0.76, 1.03, 1.53, 2.03, 3.60, 6.75, 8.10. The PI/silica masterbatch was introduced into Brabender® type internal mixer at 80 °C and masticated at 30 rpm for 60 s. The ammonium salt was then added and mixing was carried out for 240 s, discharging the composite at about 90 °C. The resultant composite was finally fed at room temperature to the mixer and peroxide was added, performing the mixing at 50 °C for 120 s. Curing was carried out at 170 °C for 20 min under a pressure of 150 bar. Composites were labelled as 2HTCl-Y, where Y indicates the amount of 2HTCl expressed in phr.

Table 1
Formulations of PI based nanocomposites containing silica and OC.[a–c]

	OC-0	OC-0.5	OC-1.1	OC-1.7	OC-2.3	OC-3.4	OC-4.5	OC-8	OC-12	OC-15	OC-18
PI	100	100	100	100	100	100	100	100	100	100	100
Silica	70	70	70	70	70	70	70	70	70	70	70
OC	0	0.5	1.1	1.7	2.3	3.4	4.5	8.0	12.0	15.0	18.0

[a] OC = Mt/2HT.
[b] Amount of ingredients are indicated in phr (part per hundred rubber).
[c] Other ingredients: TESPT 7, DCUP 1.4.

Please cite this article as: Galimberti, M., et al., Reduction of filler networking in silica based elastomeric nanocomposites with exfoliated organo-montmorillonite, Appl. Clay Sci. (2016), http://dx.doi.org/10.1016/j.clay.2016.09.017

2.2.3. PI-BR-sSBR based nanocomposites containing silica and OC

Formulations are in Table 2. In the first step of the procedure, polymers were introduced into in the Banbury® type internal mixer at 60 °C and were masticated for 30 s with rotors rotating at 75 rpm. In the second step, silica or silica and OC were then added, together with silane TESPT, stearic acid and the oil, to prepare the silica based composite or the nanocomposite, respectively. Temperature was rapidly increased to 110 °C and mixing time of the second step was 240 s. The resulting masterbatches were discharged at about 110 °C, and stored at room temperature for about 16 h. Afterwards, the addition of ZnO and 6PPD was performed by mixing at 50 °C for 120 s. The remaining ingredients (S, CBS, DPG, CTP) were then added, performing a further mixing at 50 °C for 180 s. The compounds were finally homogenised by passing them 5 times on a two roll mill, with the front roll rotating at 30 rpm and the back roll at 38 rpm. Curing of the composites was carried out at 170 °C for 20 min under a pressure of 150 bar. Composites were labelled as PI-BR-sSBR-OC-X, where X indicates the amount of OC expressed in phr.

2.3. Characterization of OC and nanocomposites

2.3.1. X-Ray diffraction

Wide-angle X-ray diffraction (WAXD) patterns with nickel filtered Cu-Kα radiation were obtained in reflection, with an automatic Bruker D8 Advance diffractometer. Patterns were recorded in 2°–80° as the 2θ range, being 2θ the peak diffraction angle.

2.3.2. Transmission electron microscopy (TEM)

TEM analysis of nanocomposites was performed with a Zeiss EM 900 microscope applying an accelerating voltage of 80 kV. Ultrathin sections (about 50 nm thick) were prepared at −130 °C by using a Leica EM FCS cryoultramicrotome.

2.3.3. Mooney viscosity measurements

Mooney viscosity was determined with a Mooney MV 2000 E Viscometer from Alpha Technologies, following the experimental procedure described by ASTM D1646. In particular, tests were run at 100 °C, using a rotor with a 38.1 mm diameter rotating at 0.209 rad/s. Rubber samples were preheated for 1 min at 100 °C and the rotor was allowed to rotate for 4 min before measuring the viscosity value, indicated in Mooney Units (MU).

2.3.4. MDR rheometric analysis

It was conducted using a Monsanto MDR rheometer, the test being carried out at 170 °C, for 30 min, at an oscillation frequency of 1.66 Hz (100 oscillations per min) and an oscillation amplitude of ±0.5°. The following parameters were obtained: M_L is the minimum torque measured; M_H is the maximum torque measured; ts_x is the time needed to have a torque equal to $(M_L + x)$; t_x is the time at x% of vulcanization required to have a torque value equal to $M_L + (x/100)(M_H - M_L)$.

2.3.5. Tensile and Hardness measurements

Both of them were performed on vulcanized samples. Tensile tests were carried out according to Standard ISO 37:2005, with a dynamometer (Zwick Roell Z010) with optical extensometer. The clamps rate was 1 mm/min and the chamber load was 10 kN. Stresses at 50, 100 and 300% elongation (σ_{50}, σ_{100} and σ_{300}, respectively), stress at break (σ_b), elongation at break (ε_B) and the energy required to break were measured. The hardness in IRHD degrees (at 23 °C and at 70 °C) was measured according to Standard ISO 48:1994.

2.3.6. Dynamic mechanical measurements

2.3.6.1. In the shear mode. Monsanto R.P.A. 2000 rheometer was used. Samples were first kept in the instrument at 120 °C for 10 min. A strain sweep (0.28–25% strain) was then performed, on raw samples, at 120 °C. Afterwards, the curing was carried out at 170 °C for 30 min, with a frequency of 1.667 Hz and an angle of 6.98% (0.5 arc). Cured samples were left in the instrument for 10 min at 50 °C. Data reported in this manuscript were finally obtained with a strain sweep (0.28–25% strain) performed at 50 °C with a frequency of 1 Hz.

2.3.6.2. In the axial mode. Dynamic-mechanical properties were measured on the crosslinked elastomeric compositions using an Instron dynamic device in the traction-compression mode according to the following procedure. Specimen with a cylindrical form (length = 25 mm; diameter = 12 mm), kept at the fixed temperature (10, 23, 70 and 100 °C) for the whole duration of the test, was compression-preloaded with 25% longitudinal deformation with respect to the initial length and was then submitted to a dynamic sinusoidal strain having an amplitude of ±3.5% with respect to the length under pre-load, with a 100 Hz frequency.

3. Results and discussion

Structure of PI/OC/silica nanocomposites, whose formulations are in Table 1, was investigated by means of XRD and TEM analysis. Fig. 1 shows the XRD patterns of pristine OC clay (a) and of OC-15 nanocomposite (b).

In the pattern of pristine OC clay, (001), (002) and (003) reflections, due to periodicities perpendicular to the structural layers, are visible at 2.5, 4.7 and 7.2 as 2θ angle values. From the 2θ angle value of (001) reflection, the 001 basal spacing can be evaluated equal to 3.5 nm. In consideration of the thickness of the clay layer (≈ 1 nm) and of the length of 2HT (≈2.5 nm) (Osman et al., 2002), the tilting angle of the hydrocarbon chains in the paraffin-type arrangement can be evaluated to be not far from 60°. Reflections due to OC clay are not present in the pattern of the nanocomposite. As reported in the literature (Galimberti et al., 2007, 2011b) such amount of OC is high enough to be detectable in

Table 2
Formulations of nanocomposites based on PI, BR and sSBR with silica and OC as fillers.[a,b]

	OC-0	OC-3
sSBR	45	45
PI	25	20
BR	30	30
Silica	70	70
OC	0	3

[a] Amount of ingredients are indicated in phr.
[b] Other ingredients: TESPT 5.2, stearic acid 2, oil 25, ZnO 3, 6PPD 2, Sulphur 1.2, CBS 1.5, DPG 2, CTP 0.5.

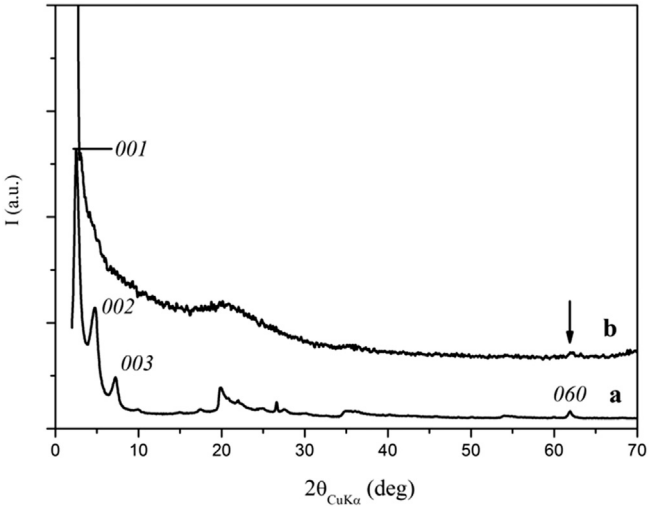

Fig. 1. XRD patterns of Mt/2HT as OC (a) and of OC-15 nanocomposite (b).

Please cite this article as: Galimberti, M., et al., Reduction of filler networking in silica based elastomeric nanocomposites with exfoliated organo-montmorillonite, Appl. Clay Sci. (2016), http://dx.doi.org/10.1016/j.clay.2016.09.017

XRD diffractograms. The absence of reflections seem thus to suggest the occurring of OC exfoliation.

TEM micrographs were taken on OC-8 and OC-15 nanocomposites and are shown in Fig. 2a,b and Fig. 2c,d, respectively.

OC distribution is similar in the two nanocomposites. In all of the micrographs, OC aggregates and isolated layers appear evenly distributed: they are visible both in the elastomer matrix and in between silica aggregates. Many isolated layers are visible at high magnification, suggesting a high level of OC exfoliation, in agreement with the results obtained from XRD analysis. The micrograph taken at high magnification on OC-15 (Fig. 2d) reveals that both layers and stacks seem to act as bridges among silica aggregates, forming an almost continuous hybrid network.

The study of the filler networking phenomenon moved from the Guth equation (Eq. (1)) (Guth, 1945a, 1945b):

$$G_c/G_m = 1 + 0.67f\Phi + 1.62f^2\Phi^2 \quad (1)$$

where G_c is the elastic modulus of the composite, G_m is the elastic modulus of the neat elastomer, Φ is the filler volume fraction and the quadratic term accounts for the mutual disturbance of filler particles. f, known as shape factor, is the ratio of length to thickness of particles or aggregates The ratio G_c/G_m is the enhancement of the neat elastomer modulus, that occurs when the elastomer is filled with rigid filler particles having largely higher elastic modulus, so that the elastic energy is stored in the elastomer. This model was applied in previous studies on nanocomposites based on Mt/2HT as the OC in NR (Ramorino et al., 2009) and in PI (Galimberti et al., 2012) as the neat polymer matrices. Initial modulus values were obtained either as the slope at the origin of stress-strain curves (Ramorino et al., 2009; Galimberti et al., 2012)

Table 3
Data of dynamic storage modulus, G', and dynamic loss modulus, G'', obtained for crosslinked OC/Silica/PI nanocomposites of Table 1.

	OC-0.5	OC-1.1	OC-1.7	OC-2.3	OC-3.4	OC-4.5	OC-8	OC-12	OC-15	OC-18
OC (phr)	0.5	1.1	1.7	2.3	3.4	4.5	8	12	15	18
$G'c$[a] (MPa)	2.9	2.9	2.9	2.8	2.8	2.9	3.2	3.4	3.6	3.6
$G'c$[a] − $G'm$[b] (MPa)	–	2.6	2.5	–	2.1	2.0	1.6	–	–	–

[a] $G'c = G'_{\gamma min}$ (0.3%) of OC-X nanocomposites.
[b] $G'm = G'_{\gamma min}$ (0.3%) of PI/Silica/2HTCl composites.

or as dynamic shear storage G' modulus at minimum deformation (Galimberti et al., 2012). Modulus enhancement as a function of the OC content was found to be strongly not linear, suggesting two different regimes for the mechanical reinforcement. By reporting the excess of modulus as a function of the OC content in a double logarithmic plot, applying the Huber-Vilgis method originally developed for CB based composites, the OC percolation threshold was calculated at about 8 phr in NR and at about 6 phr in IR.

In the present work, the filler networking phenomenon was investigated by analyzing the dependence on OC content of dynamic shear storage G' and loss G'' moduli of crosslinked nanocomposites. Crosslinking was performed with peroxide, used in place of sulphur based crosslinking system, that is known to interact with OC. The ammonium cations increase the mobility of sulphur accelerating anionic species and amines, that arise from thermal decomposition of the ammonium cations, react with sulphur (Giannini et al., 2011). Acceleration of sulphur based crosslinking reaction and increase of crosslinking network density have been documented (Avalos et al., 2008; Maiti et al.,

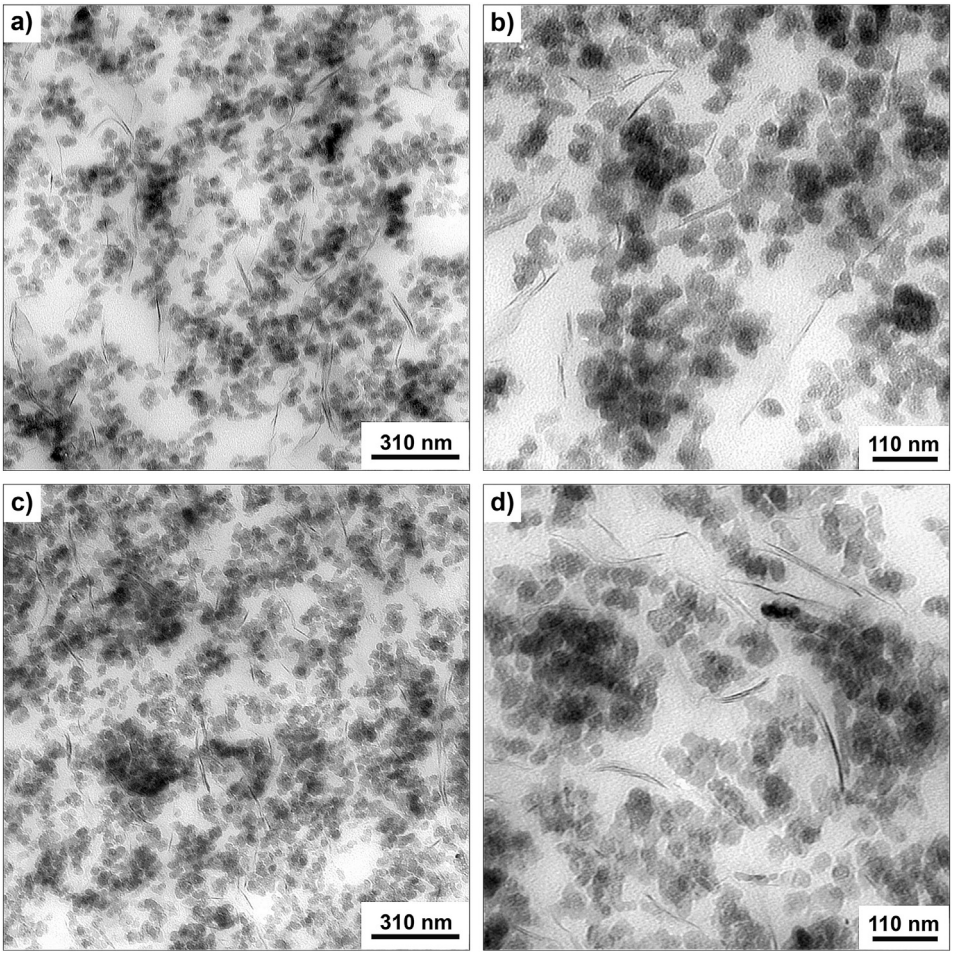

Fig. 2. TEM micrographs of OC-8 (a,b) and OC-15 (c,d) nanocomposites.

Please cite this article as: Galimberti, M., et al., Reduction of filler networking in silica based elastomeric nanocomposites with exfoliated organomontmorillonite, Appl. Clay Sci. (2016), http://dx.doi.org/10.1016/j.clay.2016.09.017

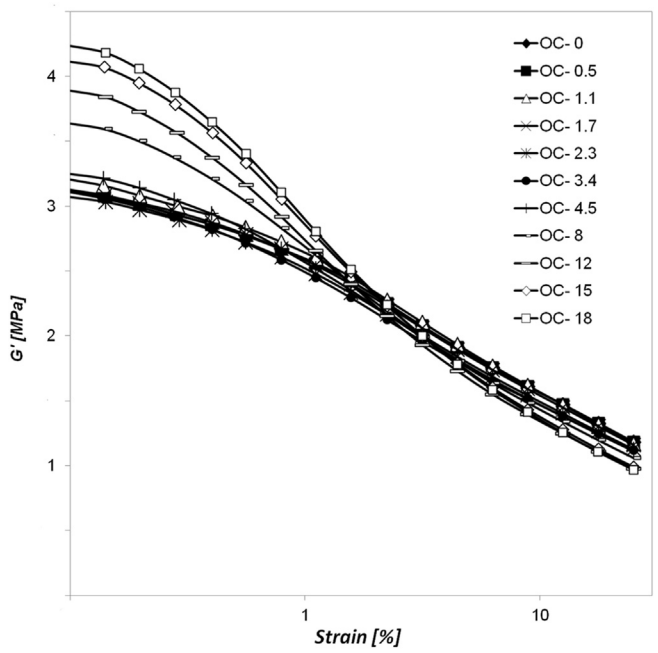

Fig. 3. Dynamic storage modulus in shear mode at 1 Hz plotted as a function of the strain amplitude for crosslinked nanocomposites of Table 1.

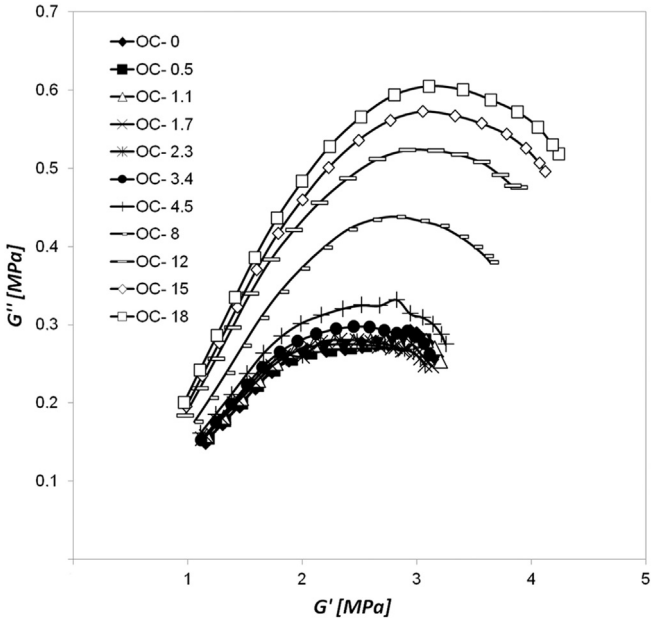

Fig. 5. Dynamic loss modulus in shear mode at 1 Hz plotted as a function of dynamic shear modulus for crosslinked nanocomposites of Table 1.

2008; Verdejo et al., 2011). $G'$and G'' moduli were measured as a function of the strain amplitude, with strain sweep tests. G' modulus at minimum deformation ($G'_{\gamma min}$) was obtained and was taken as initial modulus value. Values of $G'_{\gamma min}$ are reported in Table 3. Fig. 3 shows the dependence of G' modulus on the strain amplitude for the crosslinked nanocomposites.

It appears that curves of nanocomposites with low OC content (≤ 4.5 phr) cross over the curves of nanocomposites with higher OC content (≥8 phr), at strain amplitudes close to 5%. Moreover, crosslinking curves shown in Fig. 4 reveal that the maximum modulus M_H decreases as the OC content increases.

These findings could be interpreted considering that the lipophilic ammonium cation acts as plasticizer, reducing the modulus of the matrix. However, other hypotheses could be taken into account. OC could affect the strength of filler network and of polymer-filler interaction at high strain amplitudes. The ionic liquid could also have an effect on the efficiency of silanization. However, recently a phosphonium ionic liquid has been reported to enhance the efficiency of the silanization reaction between silica and silane TESPT, behaving as a catalyst (Tang et al., 2015)."

Fig. 5 shows, in the Cole-Cole plot, the dependence of G'' on G' modulus, for crosslinked OC-X samples.

At a given G' value, G'' values are quite similar for nanocomposites with OC content from 0.5 to 4.5 phr, whereas they appreciably and consistently increase when the OC content is at least 8 phr. This suggests that, at a given OC content, the filler networking phenomenon has a clear enhancement. The amount of OC required to have such enhancement could be estimated adopting the approach reported in the literature and commented above, correlating the initial modulus enhancement, given by the difference $\Delta G'$ between the modulus G'_c of

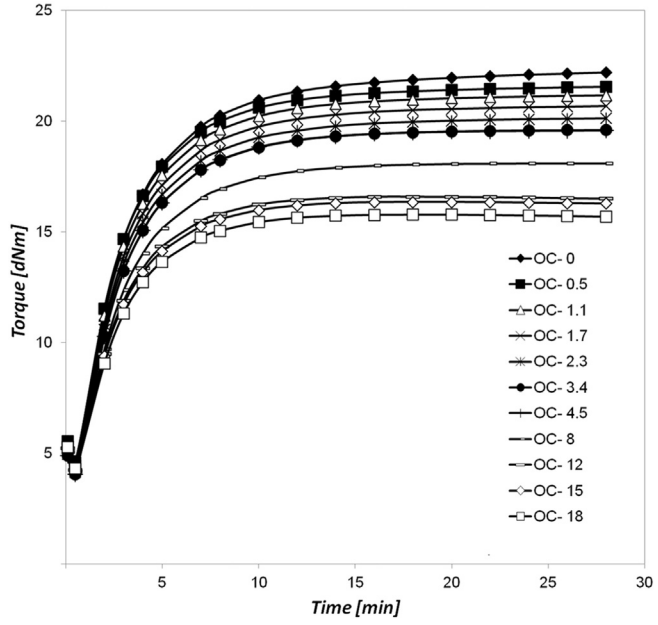

Fig. 4. Rheometer curves for nanocomposites of Table 1.

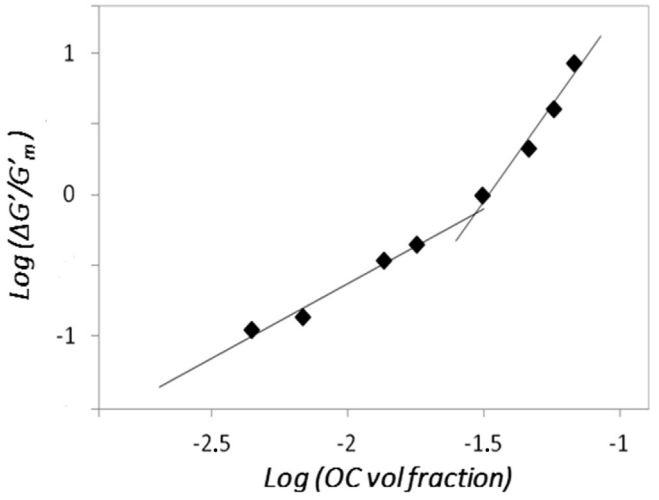

Fig. 6. Double logarithmic plot of the excess of G' modulus $\Delta G' = G'_c - G'_m$ (see text) as a function of OC volume fraction (Huber–Vilgis plot).

Please cite this article as: Galimberti, M., et al., Reduction of filler networking in silica based elastomeric nanocomposites with exfoliated organo-montmorillonite, Appl. Clay Sci. (2016), http://dx.doi.org/10.1016/j.clay.2016.09.017

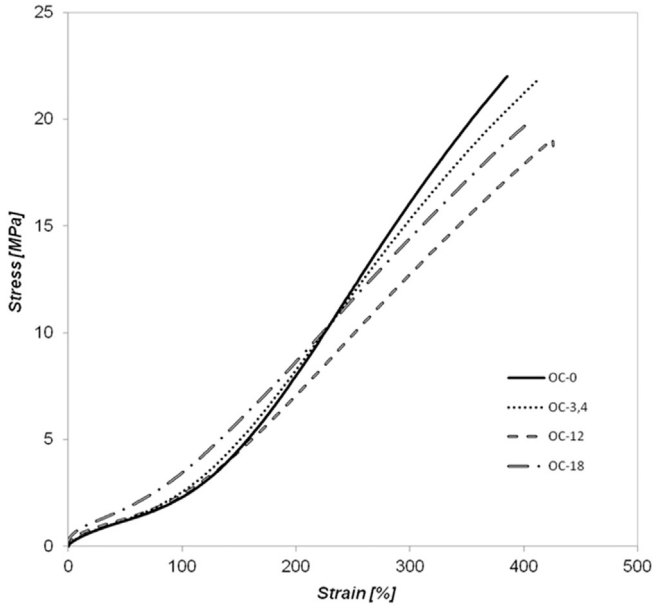

Fig. 7. Nominal stress/nominal strain curves for silica based nanocomposites of Table 1.

the composite containing OC and the modulus G'_m of the matrix ($\Delta G' = G'_c - G'_m$), with the nanofiller content. However, it is evident from what shown in Fig. 3 and in Fig. 4 that the G'_m modulus of the PI/silica composite (without OC) can not be taken as the reference modulus for all the nanocomposites. To overcome this problem, analogous composites were prepared feeding only the ammonium salt 2HTCl, in the absence of Mt. G'_m values were thus determined from strain sweep experiments in the shear mode. These experiments revealed that 2HTCl led to the reduction of G′ modulus, both at minimum and at large strain, and to the reduction of ΔG′. G′ values at minimum strain, $G'_{\gamma min}$ (0.3%), were taken as the initial modulus of the composites and were used to determine the excess of the initial modulus ΔG′. Values of the excess of modulus $\Delta G' = G'_c - G'_m$, where G'_m is the $G'_{\gamma min}$ of the neat matrix containing the ammonium salt 2HTCl, were reported in Table 3.

The Huber-Vilgis method was then applied to the hybrid filler system, by reporting the modulus excess ΔG′, as a function of OC content in a double logarithmic plot. The Huber Vilgis plot shown in Fig. 6 reveals two different regimes for the mechanical reinforcement, the switch from one to the other occurring at 7.4 phr as OC content. Such a shift could be interpreted with the formation of continuous silica-OC hybrid filler network.

This interpretation appears to be supported by the TEM micrographs shown in Fig. 2. In fact, a continuous network formed by silica and OC layers and aggregates is visible in the pictures of OC-15 (Fig. 2d).

Silica based nanocomposites presented in this manuscript have features similar to those based on CB, previously reported (Galimberti et al., 2012): they are based on the same polymer and OC, silica and CB have the same volume fraction. The existence of two regimes for the mechanical reinforcement was verified also for these OC/CB nanocomposites (Galimberti et al., 2012), and the shift from one regime to the other was found to occur for OC content of about 3 phr. Larger amount of OC is thus required to form a continuous hybrid filler network with silica rather than with CB. This finding can be justified with the dispersion of OC in silica domains, thanks to their affinity, and indicates the possibility of using larger amounts of OC without enhancing the filler networking phenomenon in silica based nanocomposites.

Tensile properties of nanocomposites of Table 1, containing 3.4, 12 and 18 phr of OC, were investigated by means of quasi-static measurements. Fig. 7 shows the obtained stress strain curves.

Nanocomposites with OC show higher break energy than the composite with only silica as the filler. The largest increase, from 34.7 to 38.3 J/cm^3, was obtained when the OC amount (3.4 phr) was below the percolation threshold. Values of initial modulus were calculated from the stress strain curves: also quasi-static measurements confirm that appreciable filler networking occurs only for OC content above the percolation threshold.

Results discussed so far show that the addition of OC to a silica based elastomeric composites leads to the improvement of the composite end properties, without affecting the dynamic-mechanical behaviour, that means without enhancing the filler networking phenomenon, provided that the OC amount is not high enough to give rise to a continuous hybrid filler network with silica.

To verify the effect of the polymer matrix on the filler networking phenomenon of OC/silica hybrid filler system, composite was prepared with a blend of PI, BR and SBR from anionic solution polymerization (sSBR). Silica was used in the same amount as in the composite discussed above and the OC content (3 phr) was lower than the one required to have the formation of the hybrid filler network. The effect of the crosslinking system was investigated by using a traditional sulphur based system, in place of peroxide. Formulations are shown in Table 3. Table 4 reports data on viscosity and parameters of the crosslinking reaction obtained for PI-BR-sSBR-OC-X samples of Table 2.

OC caused the reduction of the composite viscosity, as shown by Mooney viscosity and M_L values, whereas let the crosslinking reaction substantially unaffected. The latter finding could be due to the low amount of OC in the nanocomposite and also to the interaction of the amine arising from the ammonium decomposition with silica rather with sulphur.

Dynamic-mechanical moduli were determined in the shear mode, from strain sweep tests. G' at minimum strain ($G'_{(0.5\%)}$) and $\Delta G'_{(0.5–10\%)}$ data are in Table 5.

It is evident that OC leads to the reduction of the filler networking phenomenon.

Table 4
Viscosity data and crosslinking reaction parameters for PI-BR-sSBR-OC-X samples of Table 2.

	PI-BR-sSBR-OC-0	PI-BR-sSBR-OC-3
MU[a]	85.7	75.2
M_L [dNm]	4.2	3.3
M_H [dNm]	17.0	15.9
t_{s1} [min]	1.410	1.450
t_{90} [min]	4.790	4.200

[a] From Mooney measurements.

Table 5
$G'_{(0.5\%)}$ modulus and $\Delta G'_{(0.5–10\%)}$ for PI-BR-sSBR-OC-X samples of Table 2.

	PI-BR-sSBR-OC-0	PI-BR-sSBR-OC-3
$G'_{(0.5\%)}$ [MPa]	4.4	3.7
$\Delta G'_{(0.5–10\%)}$ [MPa]	2.9	2.2

Table 6
E', *tan* δ at different temperatures and $\Delta E'_{23–70\ °C}$ values for PI-BR-sSBR-OC-X samples of Table 2.

	PI-BR-sSBR-OC-0	PI-BR-sSBR-OC-3
E' @ 0 °C	11.7	10.9
*tan*δ @ 0 °C	0.40	0.38
E' @ 10 °C	9.6	9.2
*tan*δ @ 10 °C	0.35	0.32
E' @ 23 °C	8.3	8.0
*tan*δ @ 23 °C	0.27	0.24
E' @ 70 °C	5.9	6.0
*tan*δ 70 °C	0.17	0.16
E' @ 100 °C	5.5	5.6
*tan*δ @ 100 °C	0.16	0.13
$\Delta E'_{23–70°C}$	6.1	5.2

Please cite this article as: Galimberti, M., et al., Reduction of filler networking in silica based elastomeric nanocomposites with exfoliated organo-montmorillonite, Appl. Clay Sci. (2016), http://dx.doi.org/10.1016/j.clay.2016.09.017

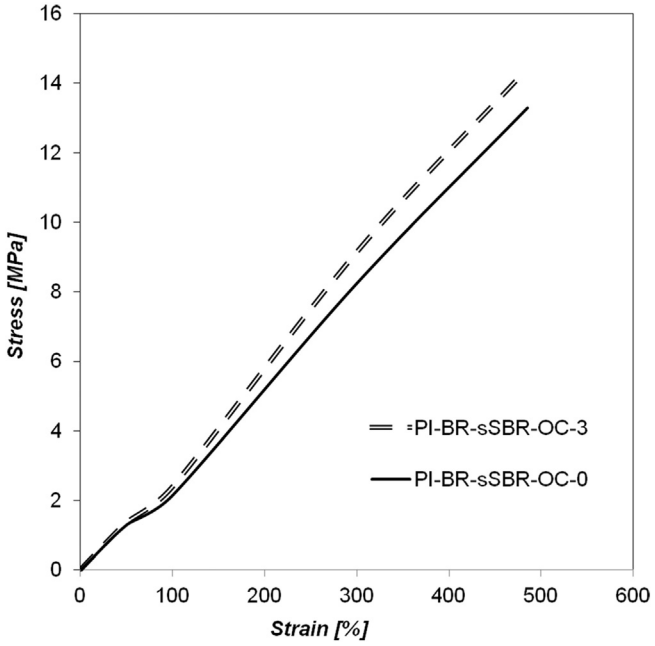

Fig. 8. Nominal stress/nominal strain curves for PI-BR-sSBR-OC-X samples of Table 2.

Dynamic-mechanical measurements were performed also in the axial mode, in wide range of temperatures, from 0 to 100 °C. Data of dynamic storage modulus (E') and loss factor ($\tan\delta$) are in Table 6.

The $tan\delta$ value is calculated as the ratio between loss (E'') and storage modulus (E'). E′ values of the OC based nanocomposite are lower at low temperatures (from 0 °C to 23 °C) and slightly higher at high temperatures (70 °C and 100 °C): the reduction of the storage modulus with the increase of temperature is more pronounced in the absence of OC. Moreover, $tan\ \delta$ values are similar at low temperatures in the absence and in the presence of OC and become appreciably lower for the OC based nanocomposite as the temperature increases. All these findings are clear indication of the reduction of the filler network, caused by OC.

Fig. 8 shows the stress strain curves for PI-BR-sSBR-OC-X samples of Table 2.

OC brought to higher stresses at all the elongations: σ_{100} was enhanced from 1.3 to 1.4 MPa and σ_{300} from 8.3 to 9.2 MPa.

Ultimate properties were improved by OC: the stress at break (σ_B) was enhanced from 13.3 to 14.2 MPa, the break energy from 29.4 to 31.7 MPa, while the elongation at break remained substantially unchanged (485 vs 477). Hardness was measured at 23 °C and 70 °C, detecting 74.3 and 71.9 as the hardness values at 23 °C for PI-BR-sSBR-OC-0 and PI-BR-sSBR-OC-3, respectively, with a reduction at 70 °C of 5.7 and 5.2 points.

All data collected for the PI-BR-sSBR-OC-X samples appear highly consistent and show that OC, used in amount lower than the one required to form the hybrid filler network with silica, in a nanocomposite crosslinked with a sulphur based system, leads to appreciable reduction of the filler networking phenomenon. To justify these results one should also take into account the role played by the ingredients, such as ZnO, stearic acid, sulphenamides, that are added to perform the sulphur based crosslinking.

4. Conclusions

This work demonstrates that the addition, to a silica based elastomeric composite, of an organically modified clay, a montmorillonite with a compensating ammonium cation bearing long chain alkenyl substituents, brings about reduction of filler networking phenomenon, lower reduction of elastic modulus as the temperature increases, improvement of stresses at every elongation and of ultimate properties such as the break energy. The ammonium cation 2HTCl, used in silica based compounds in the absence of montmorillonite, appears to be able to bring about the reduction of the filler networking, but also of the mechanical reinforcement. To achieve the abovementioned positive effects, OC should be used in a low amount, below the threshold content at which continuous hybrid OC/silica filler network is formed. Crosslinking system based on sulphur appears to be helpful, as it promotes the OC dispersion in the polymer matrix.

Results presented in this work seem to arise from the synergy among different aspects. The nanoclay promotes the mechanical reinforcement and its exfoliation allows to establish interaction between the cation bearing long chain alkenyl substituents and silica, leading to lower filler networking. The interaction between the cation and the sulphur based crosslinking system, most likely via amine formation, is likely to promote higher interface crosslinking density. The interest of results here reported is due to the great importance of silica based elastomeric composites, that are extensively used, in tyre compounds, because they allow a substantial reduction of energy dissipation and thus of fuel consumption and carbon footprint, because of the low filler networking phenomenon. The OC/silica nanocomposites studied in this work pave the way for further reduction of such phenomenon and thus for larger diffusion of silica based elastomeric composites.

References

Alexandre, M., Dubois, P., 2000. Polymer-layered silicate nanocomposites: preparation, properties and uses of a new class of materials. Mater. Sci. Eng. R 28 (1), 1–63. http://dx.doi.org/10.1016/S0927-796X(00)00012-7.

Anderson, B.J., Zukoski, C.F., 2007. Nanoparticle stability in polymer melts as determined by particle second virial measurement. Macromolecules 40 (14), 5133–5140. http://dx.doi.org/10.1021/0624346.

Annabi-Bergaya, F., 2008. Layered clay minerals: basic research and innovative composite applications. Microporous Mesoporous Mater. 107 (1–2), 141–148. http://dx.doi.org/10.1016/j.micromeso.2007.05.064.

Avalos, F., Ortiz, J.C., Zitzumbo, R., López-Manchado, M.A., Verdejo, R., Arroyo, M., 2008. Effect of montmorillonite intercalant structure on the cure parameters of natural rubber. Eur. Polym. J. 44 (10), 3108–3115. http://dx.doi.org/10.1016/j.eurpolymj.2008.07.020.

Bergaya, F., Lagaly, G. (Eds.), 2013. Handbook of Clay Science, Second Edition Elsevier, Amsterdam.

Bhattacharya, M., Bhowmick, A.K., 2010. Synergy in carbon black-filled natural rubber nanocomposites. Part I: mechanical, dynamic mechanical properties, and morphology. J. Mater. Sci. 45 (22), 6126–6138. http://dx.doi.org/10.1007/s10853-010-4699-6.

Brochard-Wyart, F., de Gennes, P., 2000. Viscosity at small scales in polymer melts. Eur. Phys. J. E 1 (1), 93–97.

Cataldo, F., 2007. Preparation and properties of nanostructured rubber composites with montmorillonite Macromol. Symposium 247, 67–77. http://dx.doi.org/10.1002/masy.200750109.

Chattopadhyay, P.K., Das, N.C., Chattopadhyay, S., 2011. Influence of interfacial roughness and the hybrid filler microstructures on the properties of ternary elastomeric composites. Compos. Part A 42 (8), 1049–1059. http://dx.doi.org/10.1016/j.compositesa.2011.04.011.

Chen, B., Evans, J.R.G., Greenwell, H.C., Boulet, P., Coveney, P.V., Bowden, A.A., Whiting, A., 2008. A critical appraisal of polymer-clay nanocomposites. Chem. Soc. Rev. 37 (3), 568–594. http://dx.doi.org/10.1039/b702653f.

Chevalier, Y., Morawski, J.C., 1984. EP 0157703 Precipitated Silica With Morphological Properties, Process for Producing it and its Application, Especially as a Filler.

Das, A., Stoeckelhuber, K.W., Rooj, S., Wang, D.Y., Heinrich, G., 2010. Synergistic effects of expanded nanoclay and carbon black on natural rubber compounds. Kautsch. Gummi Kunstst. 63 (7–8), 296–302.

Donnet, J.B., Custodero, E., 2005. Reinforcement of elastomers by particulate fillers. In: Mark, J.E., Erman, B., Eirich, F.R. (Eds.), The Science and Technology of Rubber, Third Ed Elsevier Academic Press, Amsterdam, pp. 367–400.

Feller, J.F., Bruzaud, S., Grohens, Y., 2004. Influence of clay nanofiller on electrical and rheological properties of conductive polymer composite. Mater. Lett. 58 (5), 739–745. http://dx.doi.org/10.1016/j.matlet.2003.07.010.

Flores, F., Graebling, D., Allal, A., Guerret-Piecourt, C., 2007. Modelization of flow electrification in a polymer melt. J. Phys. D. Appl. Phys. 40 (9), 2911–2919. http://dx.doi.org/10.1088/0022-3727/40/9/037.

Fröhlich, J., Niedermeier, W., Luginsland, H.D., 2005. The effect of filler-filler and filler-elastomer interaction on rubber reinforcement. Compos. Part A 36 (4), 449–460. http://dx.doi.org/10.1016/j.compositesa.2004.10.004.

Galimberti, M. (Ed.), 2011a. Rubber Clay Nanocomposites – Science, Technology, Applications. Wiley and Sons, New York.

Galimberti, M., Lostritto, A., Spatola, A., Guerra, G., 2007. Clay delamination in hydrocarbon rubbers. Chem. Mater. 19 (10), 2495–2499. http://dx.doi.org/10.1021/cm062782m.

Please cite this article as: Galimberti, M., et al., Reduction of filler networking in silica based elastomeric nanocomposites with exfoliated organo-montmorillonite, Appl. Clay Sci. (2016), http://dx.doi.org/10.1016/j.clay.2016.09.017

Galimberti, M., Riccio, P., Giudice, S., Citterio, A., Riccò, T., Pandini, S., Ramorino, G., 2009. Nanofillers for elastomers. Proceedings of the Fall 176th Technical Meeting of the Rubber Division of the American Chemical Society. Pittsburgh, USA, October.

Galimberti, M., Cipolletti, V., Giudice, S., 2011b. Morphology of rubber clay nanocomposites. In: Galimberti, M. (Ed.), Rubber Clay Nanocomposites-Science, Technology and Applications. Wiley and Sons, New York, pp. 181–240.

Galimberti, M., Coombs, M., Cipolletti, V., Riccio, P., Ricco`, T., Pandini, S., Conzatti, L., 2012. Enhancement of mechanical reinforcement due to hybrid filler networking promoted by an organoclay in hydrocarbon-based nanocomposites. Appl. Clay Sci. http://dx.doi.org/10.1016/j.clay.2012.04.019 65–66 57–66.

Galimberti, M., Cipolletti, V., Coombs, M., 2013a. Application of clay polymer nanocomposites. In: Bergaya, F., Lagaly, G. (Eds.), Handbook of Clay Science, Second Edition, Part B: Techniques and Applications. Elsevier, Amsterdam, pp. 539–586.

Galimberti, M., Coombs, M., Cipolletti, V., Riccò, T., Agnelli, S., Pandini, S., 2013b. The role of nanofillers in promoting hybrid filler networking and synergism with carbon black in a hydrocarbon rubber. Kautsch. Gummi Kunst. 7–8 31–36.

Gates, W.P., 2004. Crystalline swelling of organo-modified clays in ethanol-water solutions. Appl. Clay Sci. 27 (1–2), 1–12. http://dx.doi.org/10.1016/j.clay.2003.12.001.

Giannini, L., Citterio, A., Galimberti, M., 2011. Chemistry of rubber-organoclay nanocomposites. In: Galimberti, M. (Ed.), Rubber Clay Nanocomposites – Science, Technology, Applications. Wiley and Sons, New York, pp. 127–146.

Gopi, J.A., Patel, S.K., Chandra, A.K., Tripathy, D.K., 2011. SBR-clay-carbon black hybrid nanocomposites for tire tread application. J. Polym. Res. 18 (6), 1625–1634. http://dx.doi.org/10.1007/s10965-011-9567-9.

Guth, E., 1945a. Theory of filler reinforcement. J. Appl. Phys. 16 (1), 20–25. http://dx.doi.org/10.1063/1.1707495.

Guth, E., 1945b. Theory of filler reinforcement. Rubber Chem. Technol. 18 (3), 596–604. http://dx.doi.org/10.5254/1.3546754.

Kim, W.S., Lee, D.H., Kim, I.J., Son, M.J., Kim, W., Cho, S.G., 2009. SBR/organoclay nanocomposites for the application on tire tread compounds. Macromol. Res. 17 (10), 776–784.

Kim, W.S., Paik, H.J., Bae, J.W., Kim, W., 2011. Effect of polyethylene glycol on the properties of styrene-butadiene rubber/organoclay nanocomposites filled with silica and carbon black. J. Appl. Polym. Sci. 122 (3), 1766–1777. http://dx.doi.org/10.1002/app.34120.

Kim, W.S., Jang, S.H., Kang, Y.G., Han, M.H., Hyun, K., Kim, W., 2013. Morphology and dynamic mechanical properties of styrene–butadiene rubber/silica/organoclay nanocomposites manufactured by latex method. J. Appl. Polym. Sci. 128 (4), 2344–2349. http://dx.doi.org/10.1002/app.38253.

Konishi, Y., Cakmak, M., 2005. Structural hierarchy developed in injection molding of nylon 6/clay/carbon black nanocomposites. Polymer 46 (13), 4811–4826. http://dx.doi.org/10.1016/j.polymer.2005.03.082.

Kvande, I., Oye, G., Hammer, N., Rønning, M., Raaen, S., Holmen, A., Sjoblom, J., Chen, D., 2008. Deposition of Au colloids on plasmachemically modified carbon nanofibers. Carbon 46 (5), 759–765. http://dx.doi.org/10.1016/j.carbon.2008.01.033.

Lagaly, G., Ogawa, M., Dekany, I., 2013. Clay mineral–organic interactions. In: Bergaya, F., Lagaly, G. (Eds.), Handbook of Clay Science, Second Edition, Part A: Fundamentals. Elsevier, Amsterdam, pp. 435–505.

LeBaron, P.C., Wang, Z., Pinnavaia, T.J., 1999. Polymer-layered silicate nanocomposites: an overview. Appl. Clay Sci. 15 (1–2), 11–29. http://dx.doi.org/10.1016/S0169-1317(99)00017-4.

Leblanc, J.L., 2002. Rubber-filler interactions and rheological properties in filled compounds. Prog. Polym. Sci. 27 (4), 627–687. http://dx.doi.org/10.1016/S0079-6700(01)00040-5.

Legrand, A.P., 1998. On the silica edge. In: Legrand, A.P. (Ed.), The Surface Properties of Silicas. Wiley and Sons, New York, pp. 1–20.

Lin, J.J., Chu, C.C., Chiang, M.L., Tsai, W.C., 2006. First isolation of individual silicate platelets from clay exfoliation and their unique self-assembly into fibrous arrays. J. Phys. Chem. B 110 (37), 18115–18120. http://dx.doi.org/10.1021/jp0636773.

Maiti, M., Sadhu, S., Bhowmick, A.K., 2005. Effect of carbon black on properties of rubber nanocomposites. J. Appl. Polym. Sci. 96 (2), 443–451. http://dx.doi.org/10.1002/app.21463.

Maiti, M., Bhattacharya, M., Bhowmick, A.K., 2008. Elastomer nanocomposites. Rubber Chem. Technol. 81 (3), 384–469. http://dx.doi.org/10.5254/1.3548215.

Malas, A., Das, C.K., 2012. Carbon black–clay hybrid nanocomposites based upon EPDM elastomer. J. Mater. Sci. 47 (4), 2016–2024. http://dx.doi.org/10.1007/s10853-011-6000-z.

Osman, M.A., Ernst, M., Meier, B.H., Suter, U.W., 2002. Structure and molecular dynamics of alkane monolayers self-assembled on mica platelets. J. Phys. Chem. B 106 (3), 653–662. http://dx.doi.org/10.1021/jp0132376.

Paul, D.R., Robeson, L.M., 2008. Polymer nanotechnology: nanocomposites. Polymer 49 (15), 3187–3204. http://dx.doi.org/10.1016/j.polymer.2008.04.017.

Payne, A.R., 1962. The dynamic properties of carbon black-loaded natural rubber vulcanizates, part I. J. Appl. Polym. Sci. 6 (19), 57–63. http://dx.doi.org/10.1002/app.1962.070061906.

Praveen, S., Chattopadhyay, P.K., Albert, P., Dalvi, V.G., Chakraborty, B.C., Chattopadhyay, S., 2009. Synergistic effect of carbon black and nanoclay fillers in styrene butadiene rubber matrix: development of dual structure. Compos. Part A 40 (3), 309–316. http://dx.doi.org/10.1016/j.compositesa.2008.12.008.

Ramorino, G., Bignotti, F., Pandini, S., Riccò, T., 2009. Mechanical reinforcement in natural rubber/organoclay nanocomposites. Comput. Sci. Technol. 69 (7–8), 1206–1211. http://dx.doi.org/10.1016/j.compscitech.2009.02.023.

Rattanasom, N., Prasertsri, S., 2012. Mechanical properties, gas permeability and cut growth behaviour of natural rubber vulcanizates: influence of clay types and clay/carbon black ratios. Polym. Test. 31 (5), 645–653. http://dx.doi.org/10.1016/j.polymertesting.2012.04.001.

Ray, S.S., Okamoto, M., 2003. Polymer/layered silicate nanocomposites: a review from preparation to processing. Prog. Polym. Sci. 28 (11), 1539–1641. http://dx.doi.org/10.1016/j.progpolymsci.2003.08.002.

Sabah, E., Mart, U., Cinar, M., Celik, M.S., 2007. Zeta potentials of sepiolite suspensions in concentrated monovalent electrolytes. Sep. Sci. Technol. 42 (10), 2275–2288. http://dx.doi.org/10.1080/15275920701313616.

Sridhar, V., Shanmugharaj, A.M., Kim, J.K., Tripathy, D.K., 2009. Optimization of carbon black and nanoclay filler loading in chlorobutyl vulcanizates using response surface methodology. Polym. Compos. 30 (6), 691–701. http://dx.doi.org/10.1002/pc.20560.

Tang, Z., Huang, J., Wu, X., Guo, B., Zhang, L., Liu, F., 2015. Interface engineering toward promoting silanization by ionic liquid for high-performance rubber/silica composites. Ind. Eng. Chem. Res. 54, 10747–10756. http://dx.doi.org/10.1021/acs.iecr.5b03146.

Verdejo, R., Hernandez, M., Bitinis, N., Kenny, J.M., Lopez-Manchado, M.A., 2011. Vulcanization characteristics and curing kinetic of rubber/organoclay nanocomposites. In: Galimberti, M. (Ed.), Rubber Clay Nanocomposites - Science, Technology and Applications. Wiley and Sons, New York, pp. 275–304.

Xu, R., Wu, C., Xu, H., 2007. Particle size and zeta potential of carbon black in liquid media. Carbon 45 (14), 2806–2809. http://dx.doi.org/10.1016/j.carbon.2007.09.010.

Please cite this article as: Galimberti, M., et al., Reduction of filler networking in silica based elastomeric nanocomposites with exfoliated organo-montmorillonite, Appl. Clay Sci. (2016), http://dx.doi.org/10.1016/j.clay.2016.09.017